

The bio-organometallic chemistry of active site iron in hydrogenases[☆]

Marcetta Y. Darensbourg *, Erica J. Lyon, Jason J. Smee

Department of Chemistry, Texas A&M University, College Station, TX 77843, USA

Received 10 September 1999; received in revised form 29 November 1999; accepted 29 November 1999

Contents

Abstract	534
1. Introduction	534
1.1. Active site structures of hydrogenases from protein crystal structures and IR spectroscopy	535
1.2. General features of the six active site structures.	538
1.3. Questions arising from the active site construction and function	539
2. Modeling the Fe(CN) ₂ (CO) unit of [NiFe] hydrogenase	539
2.1. Mononuclear complexes: (η ⁵ -C ₅ H ₅)Fe(CN) ₂ (CO) [−] and derivatives.	540
2.2. Iron carbonyls in thiolate donor coordination complexes	542
2.3. NiFe heterodinuclear complexes.	544
3. Models of the diatomic ligand coordinated diiron unit of Fe-only hydrogenase	546
3.1. The organometallics, (μ-SR) ₂ Fe ₂ (CO) ₆ (Seyferth, Hieber, and Dahl chemistry).	546
3.2. (μ-SCH ₂ CH ₂ CH ₂ S) ₂ Fe ₂ (CO) ₆ and cyano derivatives	546
3.3. (μ-SR)(μ-CO)Fe ₂ organometallics	548
3.4. Reactivity of the (μ-SR) ₂ Fe ₂ unit	550

Abbreviations: CODH, carbon monoxide dehydrogenase; Cp, cyclopentadienyl; Cp*, pentamethylcyclopentadienyl; *C. pasteurianum*, *Clostridium pasteurianum* fermentative bacterium; *C. vinosum*, *Chromatium vinosum* photosynthetic bacterium; *D. gigas*, *Desulfovibrio gigas* sulfate reducing bacterium; *D. desulfuricans*, *Desulfovibrio desulfuricans* sulfate reducing bacterium; *D. vulgaris*, *Desulfovibrio vulgaris* Hildenborough strain sulfate reducing bacterium; *D. vulgaris* Miyazaki F, *Desulfovibrio vulgaris* Miyazaki F strain sulfate reducing bacterium; *D. baculatum*, *Desulfomicrobium baculatum* sulfate reducing bacterium; *T. roseopersicina*, *Thiocapsa roseopersicina* photosynthetic bacterium; XAS, X-ray absorption spectroscopy.

[☆] Note: The term ‘model’ is used in several contexts in this review: as a discrete molecule that serves as a mimic of some aspect of the active site; as a hypothesis for an arrangement of atoms which might fit observed electron density in order for the crystallographer to refine a structure; as a proposed reaction path that might serve as the mechanism for the enzyme.

* Corresponding author. Tel.: +1-409-845 5417; fax: +1-409-845 0158.

E-mail address: marcetta@mail.chem.tamu.edu (M.Y. Darensbourg).

4. Functional and theoretical modeling of [MFe] hydrogenases	552
4.1. Homolytic and heterolytic cleavage mechanisms for dihydrogen activation by metals . .	552
4.2. Functional models for heterolytic H ₂ cleavage.	553
4.3. Theoretical models for [NiFe] hydrogenase	555
5. Comments	558
Acknowledgements	558
References	558

Abstract

The recent X-ray crystal structure determinations of several hydrogenase enzymes have engaged the organometallic community owing to the presence of CN[−] and CO ligands bound to iron in the active sites. This review focuses primarily on the structural features of these metalloproteins and discusses synthetic efforts to develop small molecule models of the active sites. Specific attention is given to the use of infrared spectroscopy as an additional tool to probe different enzyme states. In addition, structurally dissimilar complexes which show some ability to facilitate either dihydrogen uptake or production, are reviewed as possible functional models. Insights from earlier work with metal hydride chemistry and recent theoretical studies are discussed in terms of functional mechanistic proposals. © 2000 Elsevier Science S.A. All rights reserved.

Keywords: Bioinorganic; Bioorganometallic chemistry; IR spectroscopy; Hydrogen activation; Hydrogenase; Synthetic models

1. Introduction

Hydrogenase enzymes are present as necessary components of many microorganisms (bacteria and archaeobacteria) which perform fundamental chemical processes of small molecule fixation and hydrogenation, or the degradation by reduction of simple oxidized species (Fig. 1) [1–3]. Hydrogenases have the ability to control H₂ concentration and reduction activity by facilitating (1) the uptake and oxidation of H₂ to protons with release of electrons; or (2) when required, its production according to the reverse reaction (Fig. 1). Possibly being the most ancient of life forms, and evolving when the earth was still in a reducing environment, these microorganisms grow best under dark and anaerobic conditions. Thus, the hydrogenase enzymes isolated from them are also oxygen and light sensitive, displaying such characteristics as are typical of many organometallic compounds.

All of the known (on the order of 80) hydrogenase enzymes are rich in sulfur and in iron; they are classified according to their metal content (Fig. 1), [NiFe], [NiFeSe], and Fe-only H₂ases. In addition, a metal-free hydrogenase is known [4,5]. The most common hydrogenase, [NiFe], containing one nickel and 12 iron atoms, and operative in all methane-producing bacteria, is also the most studied. Several excellent reviews are available [6–9] which chronicle a 25-year odyssey of biological, biophysical, biochemical and structural studies that was distinguished in 1995

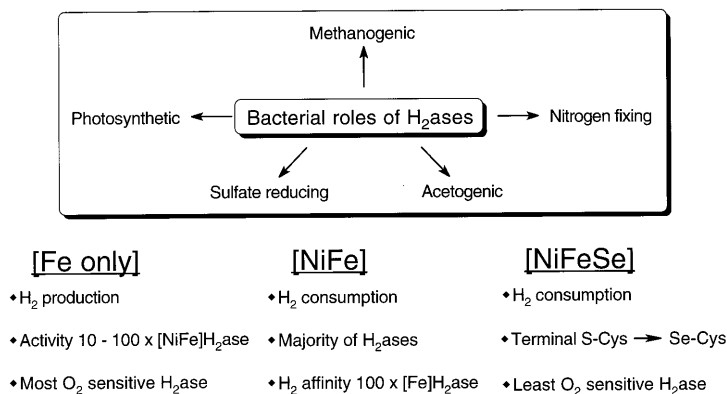


Fig. 1. Selected set of biological processes that utilize H₂ases and characteristics of the metal-containing H₂ases.

with an impressive protein crystal structure of the [NiFe]H₂ase enzyme as isolated from the sulfate reducing bacterium *Desulfovibrio gigas*, vide infra [10].

1.1. Active site structures of hydrogenases from protein crystal structures and IR spectroscopy

As of this writing, six protein crystal structures of [NiFe]H₂ase and Fe-only H₂ase metalloproteins have been determined and published, providing snapshots of unprecedented catalytic sites, isolated within the folds of a protein [10–16]. That the H₂ metabolism reactivity may be connected to such reactions as CO₂ reduction and methane or acetic acid production, for example, foretold the possibility of organometallic type reaction intermediates. That actual organometallic functionalities were found in the active sites of the six structures presented in Figs. 2 and 3 confounded all (perhaps save one group [17]) of the metalloprotein researchers, and, of course, delighted the organometallic community. Three structures are of [NiFe]H₂ases; two of these are in 'as isolated' or oxidized and enzymatically inactive forms. The [NiFeSe]H₂ase active site from the sulfate-reducing *Desulfomicrobium baculatum* bacterium, shows the seleno-cysteine to replace a terminal cysteine on nickel. Since it is less air sensitive than its thiocysteine analog, it was isolated in reduced and enzymatically active form [12]. It is thus assumed to also represent the reduced form of [NiFe]H₂ase. The Miyazaki F proteins were isolated both aerobically and anaerobically, thus giving a second reduced form for comparison to the oxidized form [13,14]. Both Fe-only H₂ase structures are presumed to be from oxidized forms of the proteins [15,16].

Whereas all hydrogenases perform the H₂ uptake/production reversibly, responding to requirements of the particular bacterial process, in general the [NiFe]H₂ases have greater reaction rates for H₂ consumption while the Fe-only are faster for H₂ production [18]. The extreme air sensitivity of the Fe-only H₂ases, coupled with the wide-spread assumption that all iron atoms were present in typical iron–sulfur

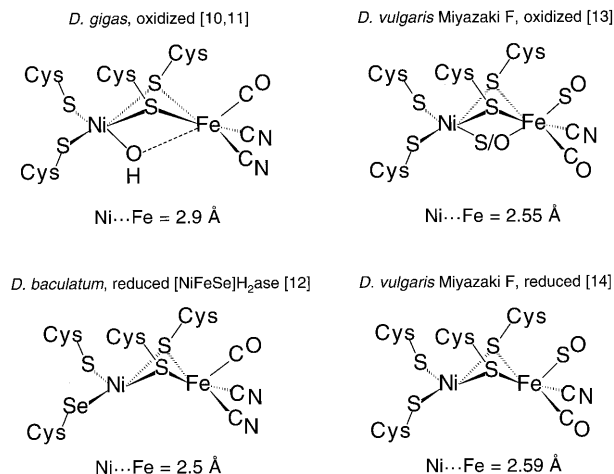


Fig. 2. [NiFe] dinuclear active sites determined from protein crystal structures.

clusters, are among the reasons that knowledge of the Fe-only enzymes is at a more rudimentary level than that of the [NiFe]H₂ases. A definitive review by Adams in 1990 clearly laid out a major gap in understanding the EPR and Mössbauer signatures of the so-called H-cluster, accepted to be the active site for H₂ production, and at the time suggested to be some form of a [6Fe6S] cluster [18]. As shown from two crystal structures (Fig. 3) this cluster is actually a dinuclear iron site, cysteine bridged (or 'hard-wired') to the first of a series of [4Fe4S] clusters which link the active site to the electron donor site external to the protein [15,16]. Such a chain of iron–sulfur clusters for electron transport is a hallmark of all the H₂ase protein crystal structures and emphasizes the importance of the inorganic mineral component of these remarkable materials.

The aforementioned general reviews are of the work of biologists, biophysicists, and biochemists long involved in the hydrogenase enzyme field. They describe classical biochemical and spectroscopic techniques which have included a primary role of electron paramagnetic resonance spectroscopy to delineate different levels of oxidation/reduction of the enzymes, which correlate with enzyme activity. While

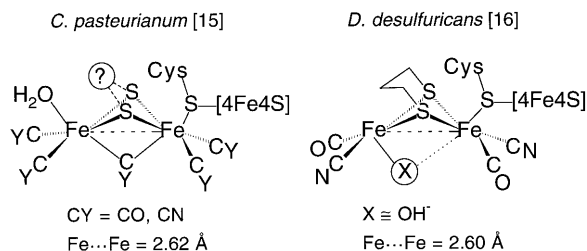


Fig. 3. Diiron active sites of Fe-only hydrogenases from protein crystallography.

implicated in the protein crystal structures, identification of the triply-bonded diatomic ligands in the active sites necessitated the use of vibrational spectroscopy to distinguish amongst reasonable possibilities: NO, CO and CN^- . The seminal IR spectroscopic study for $[\text{NiFe}]\text{H}_2\text{ase}$ from *Chromatium vinosum*, pursued on earlier observations of absorptions in the 2000 cm^{-1} region [17] and used isotopic label shifts in enzyme harvested from bacteria grown on C-13 and N-15 enriched media to assign the bands to CO and CN^- [19,20]. Thus, the stick drawing of the active site as derived from the X-ray crystal structure of oxidized *D. gigas* $[\text{NiFe}]\text{H}_2\text{ase}$ (Fig. 2) identifies the diatomics as two cyanides and one carbonyl, in agreement with the IR spectroscopy [21,22], as well as the distinct H-bonding to two of the ligands. The available IR spectroscopic studies of the *D. vulgaris* Fe-only H_2ase [23,24] lend confidence to the assignment of CO and CN^- ligands in the dinuclear active site as shown in the *D. desulfuricans* structure (Fig. 3). Vibrational studies of the Fe-only H_2ases from different organisms and in different redox states are not extensive, nor have the definitive isotopic labeling experiments been done on any Fe-only H_2ase . It has been noted that the similarity of peptide sequence at the H-cluster in the different Fe-only H_2ases suggests similar active sites [16].

The importance of development of vibrational spectroscopy as an additional probe of enzyme form and catalytic activity is emphasized in a comparison of states of *D. gigas* $[\text{NiFe}]\text{H}_2\text{ase}$ redox poised to produce various enzyme activity levels and characteristic EPR signatures [22]. Notably, as shown in Fig. 4, an oxidized form of *D. gigas* $[\text{NiFe}]\text{H}_2\text{ase}$, whose EPR signal has been designated as Ni–A, and a reduced, enzymatically active form, Ni–C, have IR spectra in the diatomic region that are extremely similar. An EPR silent form, Ni–SI, is intermediate in oxidation level but shows a complex IR pattern, possibly indicative of a mixture of diamagnetic forms. Isotopic labeling with ^{61}Ni established that the EPR signals of Ni–A and Ni–C are nickel based. The challenge to synthetic chemists of a decade ago, was to produce a model complex that simultaneously displayed easy accessibility to the $\text{Ni}^{\text{II/I}}$ and $\text{Ni}^{\text{II/III}}$ redox couples, ca. 100 and ca. 350 mV, respectively. This very narrow electrochemical range, ca. 200 mV, is in fact impossible for a single ligand set as the donor features that stabilize Ni^{I} destabilize Ni^{III} by ca. 2 V. Thus a ‘two-state’ model has been espoused by Maroney et al., deriving from results of XAS [6,25]. Small changes in the Ni K-edge energy throughout the enzymatic states were interpreted as Ni existing in only two oxidation states. Mechanistic and recent theoretical models currently assume those states are Ni^{III} and Ni^{II} , vide infra.

Similar connections between spectroscopy and various states of the enzyme exist for the Fe-only H_2ase . A recent article by Popescu et al. has revisited the spectroscopy of Fe-only hydrogenase [26]. Their interpretation of Mössbauer and ENDOR spectra indicate that the $[\text{4Fe4S}]^{2+}$ cluster, proximal to the novel $[\text{2Fe2S}]$ cluster, does not change oxidation state as the enzyme is reduced and oxidized. Electron paramagnetic resonance spectra of the oxidized forms of the enzyme reveal that the $[\text{2Fe2S}]$ ‘cluster’ exhibits an $S = 1/2$ signal suggesting low spin, valence trapped $\text{Fe}^{\text{II}}\text{Fe}^{\text{III}}$. The reduced form would then consist of the EPR silent $\text{Fe}^{\text{II}}\text{Fe}^{\text{II}}$. Later in this review we will note that the organometallic binuclear $(\mu\text{-SR})_2\text{Fe}_2$ complexes that have identical Fe–Fe distances to the enzyme contain iron formally

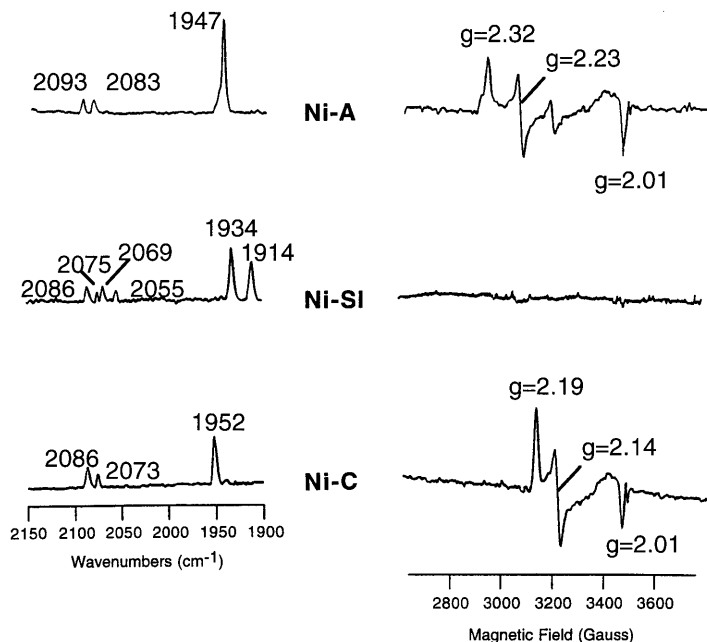


Fig. 4. A comparison of IR [22] spectra measured on *D. gigas* [NiFe] H_2 ase enzyme and EPR [27] spectra measured on *Thiocapsa roseopersicina* [NiFe] H_2 ases in three redox states: Ni-A, as isolated in an 'unready' oxidized form; Ni-SI, a reduced, diamagnetic form; and Ni-C, an enzymatically active reduced form.

in the +1 oxidation state; the possibility that the paramagnetic species is a mixed valent Fe^{II}/Fe^I was not discounted by Popescu et al.

Clearly a requirement of organometallic model complexes must be to contain analogous, well-characterized iron fragments coordinated by diatomic ligands. These will provide a basis for predictions or explanations of shifts in $\nu(CO)$ and $\nu(CN)$ values. It should be noted that as of this writing the highly unusual SO ligand which was modeled in the two structures derived from *D. vulgaris* Miyazaki F [NiFe] H_2 ase (Fig. 2) has not been corroborated by IR spectroscopy.

1.2. General features of the six active site structures

The conclusions to be drawn from the six active site structures are as follows:

- All are dinuclear, dithiolate-bridged structures with metal–metal distances typical of bonds, ca. 2.5–2.6 Å, in five of the six structures.
- Diatomic ligands, mainly CO and CN^- , are bound to iron in all structures.
- The coordination about nickel in the [NiFe] H_2 ases is pseudo-tetrahedral in the reduced enzymes while an additional bridging hydroxo, or oxo/sulfido ligand expands the nickel coordination geometry to pseudo-square pyramidal in the oxidized forms.

- The coordination about iron in the [NiFe]H₂ases is square pyramidal in the reduced forms and octahedral in the oxidized form. Octahedral geometries are also seen in the two Fe-only H₂ase structures which are presumably in oxidized enzyme states.
- Whereas both structures of Fe-only H₂ase find many similarities, the enzyme from *Clostridium pasteurianum* did not define the S to S link as a 3-carbon unit as was interpreted for the *D. desulfuricans* structure. A μ -CO bridging ligand found for *C. pasteurianum* is in accord with the IR spectrum of the oxidized form, vide infra.

1.3. Questions arising from the active site construction and function

Amongst a multitude of questions raised about the construction and function of these active sites, are the obvious: (1) Why are two metals required; two *different* metals in the case of [NiFe]H₂ases? (2) Why have the ‘abiological’ ligands, CO and CN[−], been incorporated as structural components; what are their roles? (3) Why is there such an unconventional dithiolate bridge in the Fe-only H₂ases, while the [NiFe]H₂ases demonstrate that protein-bound cysteine sulfurs are adequate to serve as bridges in the dinuclear active site?

The requirements for H₂ activation by metals are reasonably well understood by inorganic and organometallic chemists. Precedents for the function of single metal uptake and evolution of H₂ are found primarily in late and heavy transition metals that readily do two-electron oxidative addition and reductive elimination reactions. Precedents for H₂ binding as a ligand (η^2 -H₂-M complexes) and the resultant heterolytic cleavage by base into B:H⁺ and M-H[−] are also well known for d⁶ metals, vide infra. Less well defined or studied are the well known reactions of H₂ with dinuclear complexes which utilize first-row transition metals — yet these systems cut in half the drastic electronic requirements or structural rearrangements that are required at a single metal site. While structural model complexes that also have the function of hydrogenases are unknown, it is important to design similar structures in order to provide spectroscopic references. Below we describe some discrete molecules, biomimics, which provide baseline spectroscopic and chemical properties as points for consideration as mechanistic models evolve.

2. Modeling the Fe(CN)₂(CO) unit of [NiFe] hydrogenase

Outlined in Fig. 5 are characteristics expected to be of importance to the definition of the chemical reactivity of the [NiFe]H₂ase active site. While these features are intertwined and complicated beyond any single model complex, various organoiron complexes demonstrate individual required properties. More sophisticated models may result from a merger of features, however the simple, well-defined models will form the basis for spectroscopy and electrochemistry.

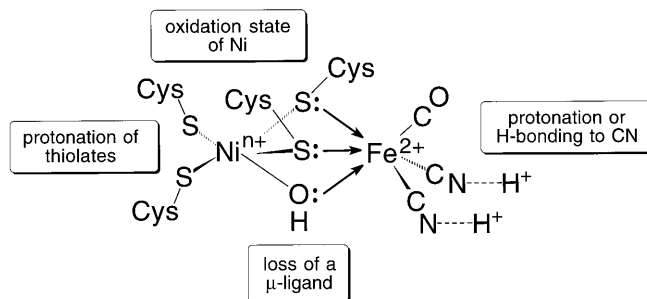


Fig. 5. Requirements for modeling the active site of [NiFe]H₂ase.

2.1. Mononuclear complexes: (η^5 -C₅H₅)Fe(CN)₂(CO)[−] and derivatives

Fig. 5 does not indicate the possibility of oxidation state changes at iron, because it is almost certain that iron remains as Fe^{II} throughout the catalytic cycle and the Fe^{II}(CN)₂(CO) pyramidal fragment remains intact throughout. This Fe^{II} fragment is found in a simple organometallic six-coordinate structure, (η^5 -C₅H₅)Fe(CN)₂(CO)[−] [28–30]. As shown in Fig. 6, its structure neatly overlays with the Fe(CN)₂(CO) moiety of the *D. gigas* enzyme, and its infrared spectrum in the diatomic region is an almost precise match of that of the enzyme as isolated (i.e.

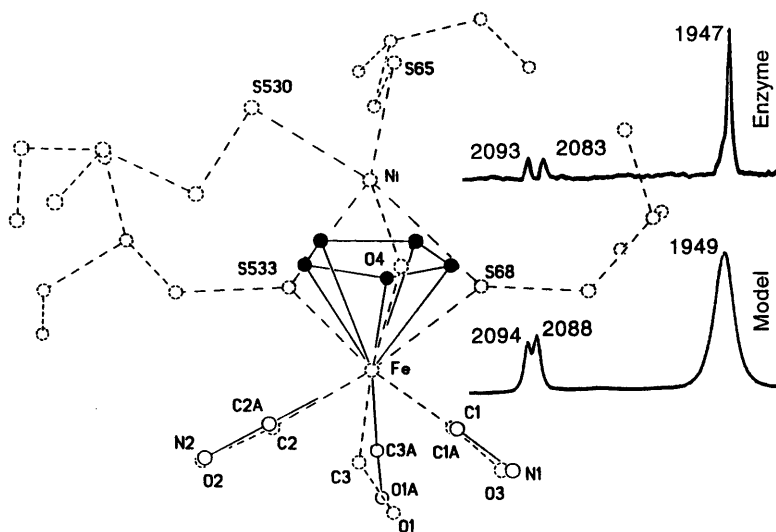


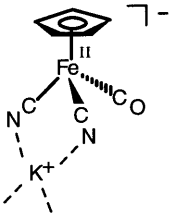
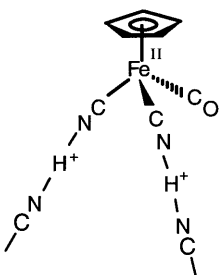
Fig. 6. Overlay of the crystal structures of the active site of *D. gigas* [NiFe]H₂ase and that of the organometallic complex anion [$(\eta^5$ -C₅H₅)Fe(CO)(CN)₂][−] with a comparison of their IR spectra.

oxidized form) from *C. vinosum* and *D. gigas* [20,22]! This match implies that the Ni-(μ -SCys)₂(μ -OH) trigonal face of the octahedral iron unit in the oxidized enzyme is a six-electron donor, anionic ligand as is the simple η^5 -C₅H₅ ring of the organometallic complex, creating the same electron density on iron as reported by the diatomic vibrational modes. It also suggests that the iron will support typical organometallic chemistry. While not ideal as a structural model, the simplicity and rigidity of the η^5 -C₅H₅ ring is advantageous in that any chemical probes or manipulations of the diatomic ligand portion of the Fe(CN)₂(CO) fragment may be carried out within a constant structural framework. This is as expected in the enzyme active site in which the cyanides are H-bonded into the protein. For example, protonation of [$(\eta^5$ -C₅H₅)Fe(CN)₂(CO)][−] produces a strong H-bonding network linking all cyanide nitrogens throughout the solid state structure (Table 1). This suggests that the protonated form contains CNH ligands [31], analogous to the CNMe ligands produced on methylation [30]. The spectral result of protonation (or methylation) is to shift the ν (CO) positively by ca. 40 cm^{−1} and the ν (CN) by +8 to +13 cm^{−1} as compared to the potassium salt of the anion when both are measured in CH₃CN solution.

To establish the sensitivity of the Fe(CN)₂(CO) unit to electron density changes both internally (change of facial donor ligand and Fe oxidation state) and externally (change of H-bonding, ion-pairing and solvent interactions) a series of nine derivatives of the Fe diatomic unit was developed for spectroscopic study [30]. This series covers a range of electronic effects (as confirmed by electrochemical studies)

Table 1

Structures, diatomic stretching frequency data, and electrochemistry of K[(η^5 -C₅H₅)FeCO(CN)₂] and its protonated form [30]

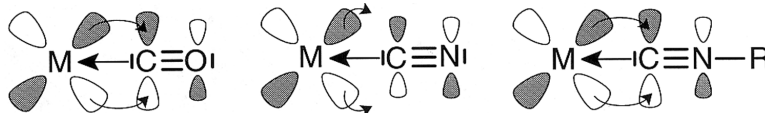
<div style="display: flex; justify-content: space-around; align-items: center;">   </div>		
Complex	K[(η^5 -C ₅ H ₅)FeCO(CN) ₂]	H[(η^5 -C ₅ H ₅)FeCO(CN) ₂]
ν (CO) ^a (cm ^{−1})	1949	1988
ν (CN) ^a (cm ^{−1})	2088, 2094	2096, 2107
Fe–CO (Å)	1.72(2)	1.75(1)
Fe–CN _(avg) (Å)	1.91(1)	1.86(1)
$E_{1/2}$ (Fe ^{II/III}) ^b (V)	+0.83	+0.95

^a Measured in CH₃CN solution.

^b Reversible couples measured in CH₃OH, referenced versus ferrocene and scaled to NHE.

within a constant hexa-coordinate structure. A primary goal was to correlate the relative responses of the CN^- and CO ligands, $\nu(\text{CO})$ and $\nu(\text{CN})$, to electronic differences in facial ligand ($\eta^5\text{-C}_5\text{H}_5$ versus $\eta^5\text{-C}_5\text{Me}_5$); alkylation, H-bonding or alkali cation ion pairing to cyanide nitrogen; and oxidation state of Fe. The $\text{Fe}^{\text{II/I}}$ reduction potentials measured for several derivatives are plotted as a function of $\nu(\text{CO})$ and $\nu(\text{CN})$ in Fig. 7. Less electron rich ligand environments are indicated by both the increase in $\nu(\text{CO})$ and $\nu(\text{CN})$ values and by the more positive E_{pc} values. While both CO and CN^- respond in the same direction, the slopes of the plots show the shift in $\nu(\text{CN})$ is about 1/3 that of $\nu(\text{CO})$. This response difference was also seen in plots of force constants, F_{CO} versus F_{CN} for seven members of the series. Again both CN^- and CO are reliable reporter ligands for electron density changes, however, the CO vibrational mode is 2.6 times more sensitive than is the CN^- , reflecting the greater ability of CO to participate in π -backbonding.

Since the intensity of $\nu(\text{CX})$ bands is a function of π -electron mobility or delocalization, information may also be gained from intensity differences in $\nu(\text{CO})$ and $\nu(\text{CN})$. Again the better π -accepting ability of CO relative to the cyanide anion shows itself in much more intense bands for the former. On protonation or alkylation however the resultant $\text{C}\equiv\text{NH}$ or $\text{C}\equiv\text{NR}$ gains in π -accepting ability and in intensity. Such intensity gains could be useful in determining the extent of H-bonding which tethers cyanides to the protein in hydrogenases.



2.2. Iron carbonyls in thiolate donor coordination complexes

Examples of diatomic ligands bound to iron in homoleptic (the same ligand) complexes are extensive and indeed such compounds serve as starting materials for the vast chemistry of organoiron compounds, i.e. iron carbonyls such as $\text{Fe}(\text{CO})_5$ and $\text{Fe}_2(\text{CO})_9$; and ferro- and ferricyanide, $\text{Fe}(\text{CN})_6^{4-}$ and $\text{Fe}(\text{CN})_6^{3-}$. Despite their

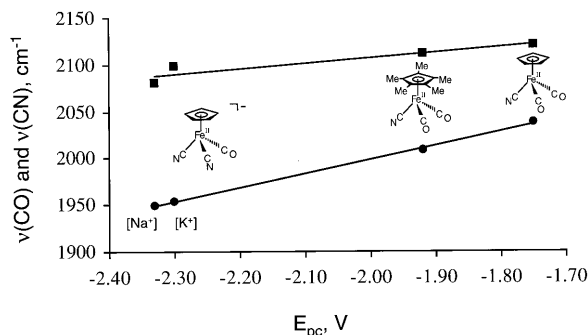
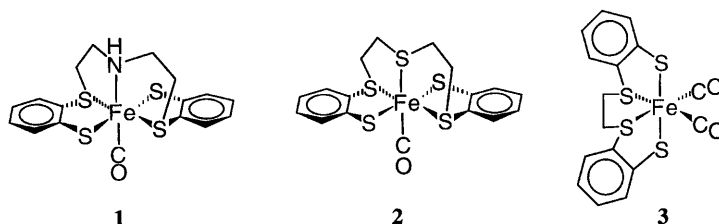


Fig. 7. Plot of $\nu(\text{CO})$ (●) and $\nu(\text{CN})$ (■) values versus $\text{Fe}^{\text{II/I}}$ reduction potential for selected derivatives of $\text{K}[(\eta^5\text{-C}_5\text{H}_5)\text{Fe}(\text{CO})(\text{CN})_2]$.

M–C bonds, the last complexes are not included as organometallic complexes, however they are known to form heteroleptic (mixed ligand) complexes such as $[\text{Fe}(\text{CN})_5\text{CO}]^{3-}$ and $[\text{Fe}(\text{CN})_5\text{NO}]^{2-}$. In addition the carbonyl rich, Fe(0) complex containing one cyanide, $\text{Fe}(\text{CO})_4(\text{CN})^-$ is known [32,33]. The incorporation of a third ligand type, the σ - and π -donating thiolate, has been accomplished as models for the iron site in $[\text{NiFe}] \text{H}_2\text{ase}$. They serve to demonstrate the effect of S-protonation on $\nu(\text{CO})$, a point that is not so pertinent to the current view of the enzyme active site since terminal thiolates are on the nickel rather than on the iron. Nevertheless they are valuable in general as spectroscopic references.

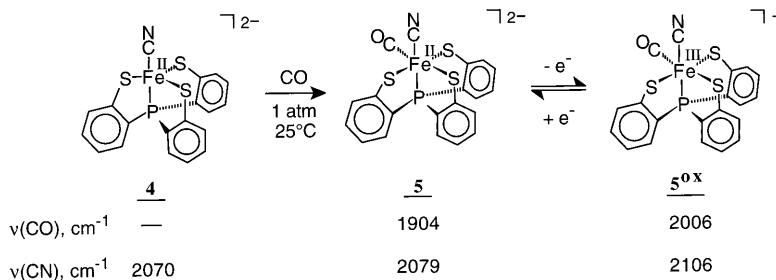
Complex **1** demonstrates the use of $\nu(\text{CO})$ as a reporter ligand for four levels of protonation of the thiolato carbonyl (Scheme 1) [34]. From the deprotonated amine anionic complex to the fully protonated dithiol, dicationic complex the $\nu(\text{CO})$ shifts positively by ca. 100 cm^{-1} . The electrochemical analysis for the series shows the $\text{Fe}^{\text{II/III}}$ couple to track the shifts in $\nu(\text{CO})$, becoming less accessible by ca. 600 mV with each level of protonation (and increase of positive charge on the complex). Concomitantly, the reduction process becomes more accessible, but is removed from the oxidation process by ca. 2 V. Sulfur alkylation of complexes **2** and **3** show similar $\nu(\text{CO})$ shifts with conversion of the dithiolates to mono- and di-thioethers [35]. The dicarbonyl complexes, **3**, **3·Et**⁺ and **3·Et**₂²⁺, have average $\nu(\text{CO})$ values ca. 60 cm^{-1} higher than the analogous single carbonyl compounds **2**, **2·Et**⁺ and **2·Et**₂²⁺, reflecting the additive electron withdrawing effects of CO ligands. Sellman et al. noted that the advantages of thiolates as ancillary ligands at redox and protonation active catalytic sites lay in their ability to facilitate uptake and release of electrons with little coordination geometry reorganization [34].



Complex **4** demonstrates the ease with which the pentacoordinate iron(II) complex can take up CO, and the resultant positive shift of $\nu(\text{CN})$ makes apparent the charge delocalization ability of CO [36]. As might be expected, a change in

	$[\text{Fe}^{\text{II}}\text{-CO}]^-$	$\xrightarrow{\text{H}^+}$	$[\text{Fe}^{\text{II}}\text{-CO}]^0$	$\xrightarrow{\text{H}^+}$	$[\text{Fe}^{\text{II}}\text{-CO}]^{1+}$	$\xrightarrow{\text{H}^+}$	$[\text{Fe}^{\text{II}}\text{-CO}]^{2+}$
	deprotonated amine 1 ⁻		1		1·H ⁺		1·(H⁺)₂
$\nu(\text{CO}), \text{cm}^{-1}$	1940		1965		1999		2044
$E_{1/2}(\text{Fe}^{\text{II/III}}), \text{V}$	N/A		+ 0.35		+ 0.98		+ 1.46

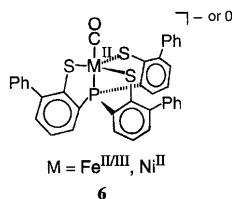
Scheme 1.



Scheme 2.

charge on complex **5** resulting from oxidation state change at the metal (Scheme 2) results in a more dramatic shift of $\nu(\text{CO})$ as compared to charge changes resulting from ligand protonation (Scheme 1). Demonstrating a $\nu(\text{CO})\text{:}\nu(\text{CN})$ response ratio of ca. 4:1, the shift in $\nu(\text{CO})$ with oxidation of Fe^{II} to Fe^{III} is $+102 \text{ cm}^{-1}$, while the shift in $\nu(\text{CN})$ is only $+27 \text{ cm}^{-1}$ [36].

While the binding of carbon monoxide to the high valent Fe^{III} in complex **5^{ox}** is unusual, it is not without precedent in Fe^{III} complexes of multi-anionic ligands. In fact the phosphinotrithiolato ligand appears to be well suited for stabilizing unusual CO binding as the ligand can support both $\text{Fe}^{\text{III}}(\text{CO})$ and $\text{Ni}^{\text{II}}(\text{CO})$ (**6**) [37]. As examples of $\text{Ni}(\text{II})$ carbonyls are limited [38,39], the later complex provides a welcome precedent for the so-called labile CO, presumed to be nickel-bound [40], in CO-inhibited $[\text{NiFe}]\text{H}_2\text{ase}$ as well as the proposed Ni–CO moiety in the carbon monoxide dehydrogenase (CODH) reaction [41].

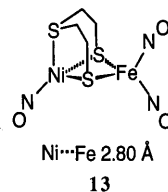
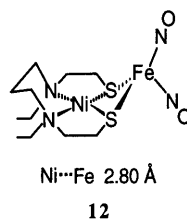
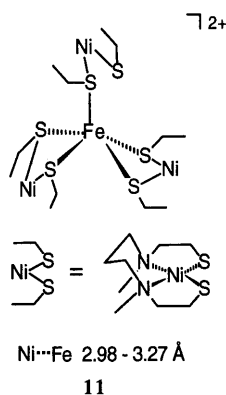
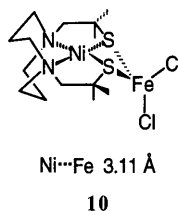
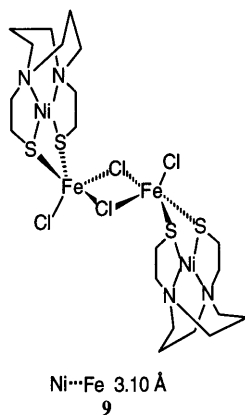
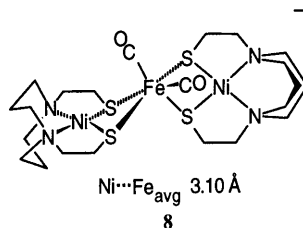
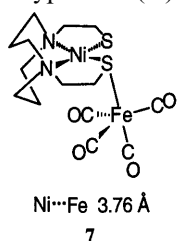


2.3. NiFe heterodinuclear complexes

The active site structure of *D. gigas* $[\text{NiFe}]\text{H}_2\text{ase}$ finds a Ni–Fe distance of 2.9 \AA closing to 2.6 \AA as the enzyme is changed from its oxidized (triply bridged) to the *D. baculatum* reduced (doubly bridged) forms [10,12]. From *D. vulgaris*, Miyazaki F, the Ni–Fe distance is 2.6 \AA in both oxidized and reduced forms [13,14]. A review of structurally characterized, thiolate-bridged NiFe heterometallic compounds, structures **7–13**, find bond distances ranging from 2.8 to 3.8 \AA . Complexes **7** and **8** use the bismercaptioethanediazacyclooctanenickel(II), (bme-daco) Ni^{II} as metallothiolate ligand to $\text{Fe}(0)$ and $\text{Fe}(\text{II})$ carbonyls, demonstrating in the case of the former, a monodentate binding and an electron donor ability to the $\text{Fe}(\text{CO})_4$ moiety much like PPh_3 [42]. On oxidation of the $\text{Fe}(0)$ in complex **7** to $\text{Fe}(\text{II})$, two (bme-daco) Ni^{II} units bind as bidentate ligands, thus producing in essence a $\text{Ni}_2\text{S}_4\text{Fe}^{\text{II}}(\text{CO})_2^{2+}$ unit. Since the Ni–Fe distances are beyond bonding range, we feel

the most reasonable view of these compounds is of metal-shared thiolates, and that each metal is influenced by the pendant metal only through the effect of charge neutralization of the thiolates. The much shorter distances found in the reduced enzyme structures suggests a greater extent of delocalization or NiFe bond character.

Examples of $\text{N}_2\text{S}_2\text{Ni}$ as a bidentate metallothiolate ligand bound to ‘organometallic’ Fe(II), complex **8** and ‘inorganic’ Fe(II), as FeCl_2 in complexes **9** [43] and **10** [44], find Ni–Fe distances of 3.10 Å, far beyond the enzyme Ni–Fe distance. Complex **11** is a unique NiFe heterometallic which uses the $\text{N}_2\text{S}_2\text{Ni}$ as both monodentate and bidentate metallothiolate ligands [45]. The shortest Ni–Fe distance found thus far, 2.8 Å, is for the $\text{Fe}(\text{NO})_2$ derivatives, complexes **12** [46] and **13** [47]. Interestingly, the former contains a typical Ni(II) and the latter is best described as $\text{Ni}(0)$. Whether the



2.8 Å distances reflect substantial metal orbital overlap in these complexes has not been determined.

The redox properties of complexes **9** and **10** were used to support a theory that the binding of Fe(II) to nickel dithiolate is a requirement for the ambiguous redox properties of [NiFe]H₂ase described above. That is, to account for the narrow potential window, the positioning of Fe(II) on and off the ‘bridging thiolates’ could serve as a redox couple switch [48]. In the on-position the pendant iron would neutralize the π -donor effects of the thiolate and shift Ni^{II/I} into the mild biological range; in the off position, the nickel could feel the full effect of four thiolates in stabilizing the Ni^{II/III} couple. With the additional crystal structures in both oxidized and reduced forms showing the Fe(CN)₂(CO) unit firmly attached to the μ -(SR)₂, this once attractive model is no longer likely.

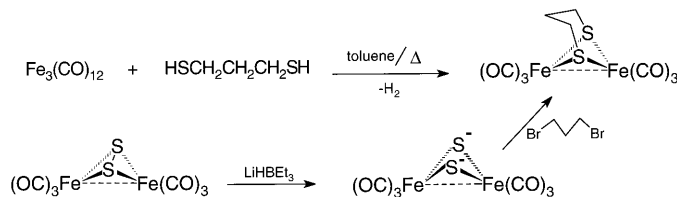
3. Models of the diatomic ligand coordinated diiron unit of Fe-only hydrogenase

3.1. The organometallics, $(\mu\text{-SR})_2\text{Fe}_2(\text{CO})_6$ (Seyferth, Hieber, and Dahl chemistry)

The diiron site in the Fe-only hydrogenase structures holds a distinct resemblance to members of a well-known series of $(\mu\text{-SR})_2\text{Fe}_2(\text{CO})_6$ and phosphine/CO-substituted derivatives [49–52]. In these dimeric, diamagnetic complexes, the $\mu\text{-SR}^-$ anion is a four-electron donor, the iron atoms are in their +1 oxidation state, and the known structures have Fe–Fe distances of 2.5–2.6 Å, well within bonding range and as predicted by the 18-electron rule. The coordination geometry about iron is described as pseudo-octahedral, with the ‘bent’ Fe–Fe bond occupying the sixth position [53]. Alternatively, description as a pseudo-square pyramid is also appropriate as the Fe is typically positioned above the best S₂(CO_{equatorial})₂ plane and displaced toward the axial CO. With SMe[−] or SEt[−] as bridging ligands, *syn* and *anti* isomers exist [54], as defined by their orientation relative to each other, and may create quite different reactivity properties, vide infra. The sulfurs may be joined by $-\text{C}_2\text{H}_4-$, $-\text{C}_3\text{H}_6-$, and other organic linkers, obviating the *syn/anti* isomer problem [55]. When carbonyls are replaced by other ligands, many isomeric forms may be produced due to the geometrically distinct coordination positions about iron [52].

3.2. $(\mu\text{-SCH}_2\text{CH}_2\text{CH}_2\text{S})_2\text{Fe}_2(\text{CO})_6$ and cyano derivatives

We have prepared the propanedithiolate (pdt) bridged diironhexacarbonyl complex according to the synthetic procedures of Scheme 3 [55–57], and compared its molecular structure to that of the Fe-only active site (Fig. 8) [58]. The Fe–Fe distance of 2.510 Å of the model complex is only 0.1 Å shorter than those reported for the diiron site of the enzyme structures (see Fig. 3). The match of the $(\mu\text{-pdt})\text{Fe}_2$ unit is excellent with the exception of the bridgehead methylene group which is somewhat restricted according to the protein structure. Alternatively this mismatch could indicate a need for the protein crystallographers to reconsider their interpretation of the S to S linker. The match of the remainder of the coordination sphere



Scheme 3.

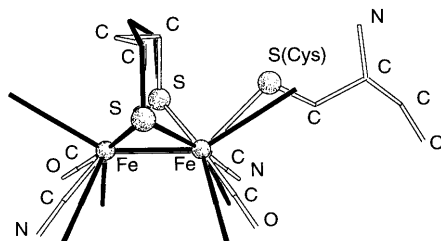


Fig. 8. Superposition of $(\mu\text{-SCH}_2\text{CH}_2\text{CH}_2\text{S})\text{Fe}_2(\text{CO})_6$ with the iron site of Fe-only hydrogenase using the protein crystal as isolated from *D. desulfuricans* (reproduced from Ref. [58]).

geometries is sufficient to suggest that the geometrical and electronic requirements of the organometallic are being met in the enzyme active site.

The incorporation of cyanide into this unit is readily accomplished according to the chemistry expressed in Fig. 9. Although the $(\mu\text{-pdt})\text{Fe}_2(\text{CO})_6$ compound is slow to exchange CO ligands with ^{13}CO , with CN^- reaction occurs readily producing the dicyano complex $(\mu\text{-pdt})\text{Fe}_2(\text{CO})_4(\text{CN})_2^-$ [58]. The expected monocyano intermediate is seen only as a transient in the IR spectrum; its identity was confirmed by the alternate route preparation using the $^-\text{N}(\text{SiMe}_3)_2$ nucleophilic reagent. Fig. 9 shows the IR spectra of parent hexacarbonyl, cyano and dicyano derivatives. It is noteworthy that the lowest $\nu(\text{CO})$ band of the dicyanodicyanide, 1883 cm^{-1} , is within 40 cm^{-1} of the lowest $\nu(\text{CO})$ band of the *D. vulgaris* enzyme, found at 1847 cm^{-1} [24]. The presence of a bridging carbonyl is not at all disputed, as we present below an example of $\text{Fe}^{\text{II}}(\mu\text{-SR})(\mu\text{-CO})\text{Fe}^{\text{II}}$ with the exact $\nu(\text{CO}_{\text{bridging}})$ value as the enzyme. However, as of this writing the isotopic labeling experiments that were so instructive for the $[\text{NiFe}]\text{H}_2\text{ase}$ enzyme structures have not been reported for the Fe-only H_2ases . The 1883 cm^{-1} CO band of the model complex reflects the electron-rich character of the iron when ligated by the two anionic cyanide ligands, shifting the lowest $\nu(\text{CO})$ band of the parent hexacarbonyl negatively by ca. 100 cm^{-1} . This is as would be expected had the anionic charge resulted from reduction of iron(I) to iron(0).

The representation of the dicyano complex in Fig. 9 shows cyanides in equatorial positions on each iron. This assignment was based on comparative $\nu(\text{CO})$ intensity data from structurally characterized bisphosphine complexes [52]. Recent X-ray structures of $[\text{PPh}_4^+]_2[\text{anti}-(\mu\text{-SMe})_2\text{Fe}_2(\text{CO})_4(\text{CN})_2^-]$ and $[\text{Et}_4\text{N}^+]_2[(\mu\text{-pdt})\text{Fe}_2-$

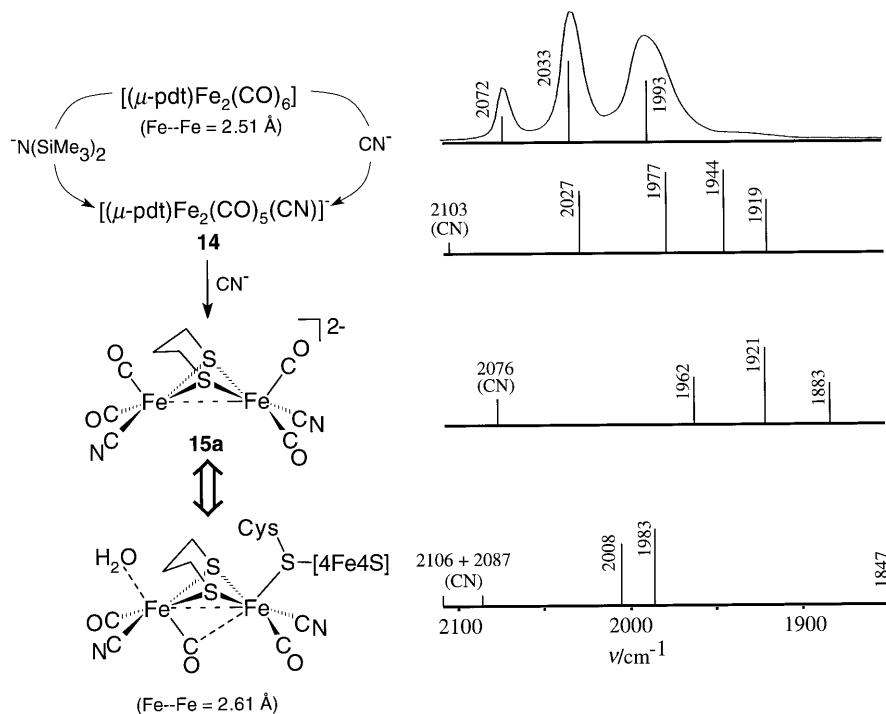
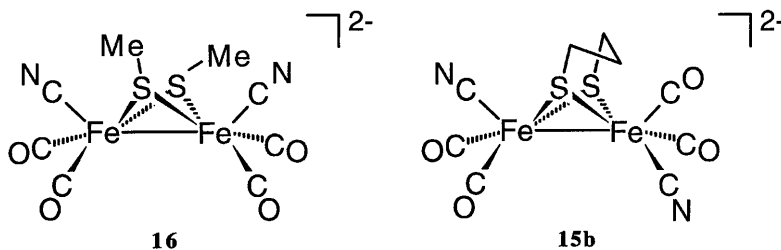


Fig. 9. CO substitution of $(\mu\text{-pdt})\text{Fe}_2(\text{CO})_6$ with CN^- and resulting IR solution spectra compared to the spectrum obtained from the oxidized form of *D. vulgaris* Fe-only hydrogenase (reproduced from Ref. [58]).

$(\text{CO})_4(\text{CN})_2^{2-}]$, complexes **16** and **15b**, respectively, indeed find one cyanide on each iron, however the former has both cyanides *cis* to the $(\mu\text{-SR})_2$ while the latter has one *cis* and one *trans* [59]. Thus for the cyanide ligands, there appears to be little site preference for axial versus equatorial in the pseudo-square pyramidal units of this type. Interestingly, in all spectra recorded thus far, there is only one CN^- stretch.



3.3. $(\mu\text{-SR})(\mu\text{-CO})\text{Fe}_2$ organometallics

Interestingly the $(\mu\text{-SR})_2(\mu\text{-CO})\text{Fe}_2$ moiety found in the oxidized form of the Fe-only H_2 ase has no analogs in the Cambridge Crystallographic Data Base,

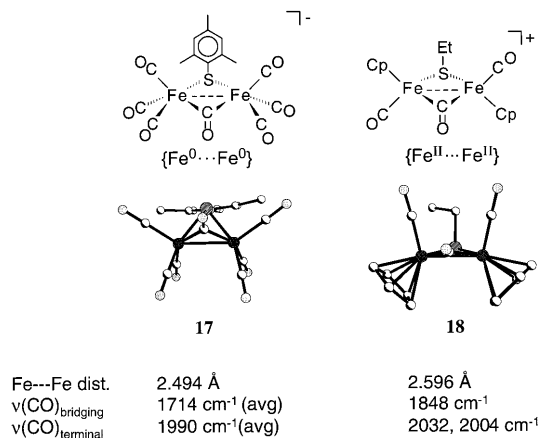
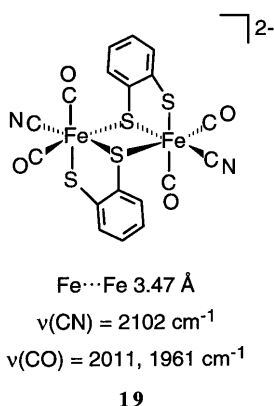


Fig. 10. Structures and IR data of dinuclear Fe⁰ and Fe^{II} complexes containing (μ-SR) and (μ-CO) [60,61]. Multiple bands were reported for the THF solution spectrum of Et₃NH[(μ-S-mesityl)(μ-CO)Fe₂(CO)₆] [61].

however ca. ten compounds with one (μ-SR) and one (μ-CO) were found. Representative examples presented in Fig. 10 find both iron(0) and iron(II) species, complexes **17** and **18**, respectively, to have similar bond distances [60,61]. The flexibility in the Fe₂(μ-SR)(μ-CO) core, as seen in Fe₂(μ-SR)₂ cores, is observed in the folding of the Fe(0) derivative as compared to the flat Fe(II) derivative. Interestingly, the $\nu(\text{CO})$ of both the bridging and terminal carbonyls of complex **18**, compares well with the values of the enzyme. In fact, it is the best spectroscopic match for $\nu(\text{CO})$ of all model complexes thus far.

Complex **18** is a rare example of a dinuclear species with an Fe^{II}...Fe^{II} distance within bonding range. A recent cyano-carbonyl Fe^{II} dimer, complex **19**, designed and produced by Liaw et al., shows the typical Fe^{II}...Fe^{II} distance of ca. 3.4 Å [62].



3.4. Reactivity of the $(\mu\text{-SR})_2\text{Fe}_2$ unit

Two types of reactivity are available to the $(\text{bridge})\text{Fe}_2(\text{CO})_6$ complexes: ligand substitution and oxidative addition. The former has provided a venue for detailed kinetic/mechanistic studies for CO substitution by phosphines in dinuclear complexes [63–65]. While associative mechanisms are appropriate to these systems, with bridge = $(\mu\text{-SR}^-)_2$ complications arise because of competing *syn/anti* interconversions of the R substituents; in one study, the *syn* isomer underwent phosphine substitution of CO with a rate 200 times that of the *anti* isomer [65]. As mentioned above, *syn/anti* isomerism is not appropriate to the small hydrocarbon linked thiolates such as ethane- or propanedithiolate. Interestingly, for both CN^- (preliminary results from our laboratories) and phosphine substitutions, the complex undergoes disubstitution, placing a substituent on each metal with such facility that the second goes on typically as rapidly as the first [64]. This result is counter intuitive for successive nucleophilic CN^-/CO displacement reactions and suggests an unexpected cooperativity within the dinuclear site.

Several bis-phosphine-substituted complexes have been used in studies of dinuclear oxidative addition; molecular structures of these such products are presented in Fig. 11. Creating triply bridged S-donor complexes from oxidative addition of SR^+ and SO_2 generates face-shared octahedra with Fe–Fe distances of $> 3.0 \text{ \AA}$, indicating the Fe–Fe ‘bond’ density has been utilized in the reduction of SR^+ and SO_2 , creating non-bonded Fe(II) sites [66,67]. In contrast, the oxidative addition of a proton into the Fe–Fe site, producing a bridging hydride, lengthens the Fe–Fe distance by only 0.08 \AA [68]. This result suggests retention of substantial delocalization of electron density in the $\text{Fe}^{\text{II}}(\mu\text{-SR})_2(\mu\text{-H}) \text{Fe}^{\text{II}}$ unit.

Before leaving this section we comment that routes to the $(\mu\text{-pdt})\text{Fe}_2(\text{CO})_6$ and analogs derive from a wealth of reactivity which provide chemically interesting

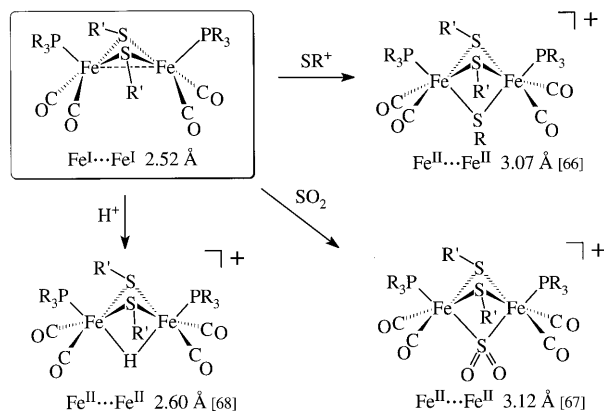


Fig. 11. Dinuclear oxidative addition reactivity as described in the Refs. indicated.

discussion points with regards to Fe-only hydrogenase. Utilizing the reducing equivalents of the Fe⁰ carbonyl precursor, addition of thiols are known to form the dinuclear complex with release of H₂ gas, as shown in Scheme 3. The alternate route which begins with the air-stable disulfide, (μ-S₂)Fe₂(CO)₆ unit reduced to the dianionic (μ-S)₂Fe₂(CO)₆²⁻, is subsequently alkylated by 1,3-dibromopropane [55–57]. Such general alkylation to bridging dithiolates is further expressed in Fig. 12 which indicates still another possibility for creating S–C bonds (via photolysis in the presence of ethylene) at the Fe₂S₂ unit [69]. The forerunner studies of Mary Rakowski-Dubois [70] of disulfide-bridged dinuclear molybdenum complexes provides precedents for reactions of ethylene and (μ-S₂)Fe₂(CO)₆ to produce the μ-ethanedithiolate bridged analog to the μ-propanedithiolate complex described above. These reactions are pointed out to express our view that nature’s engagement of the putative μ-propanedithiolate ligand to bridge two iron centers rather than calling upon two cysteinate ligands suggests that the mineral component, the Fe₂S₂ unit, is a likely candidate for the first step in the chemical genesis of this site, and may indeed be regained during the catalytic process. Fig. 12 points out that protonation of the (μ-S)₂Fe₂(CO)₆²⁻, complex **21**, leads to stable (μ-SH) derivatives, which could be an S-based site for H₂ production [71]. Carbon monoxide stabilizes the reduced states or electron rich states of this site, therefore providing an explanation for its incorporation into the active site. Cyanide may increase electron richness in a less H-bonded anionic form; or, in a strongly H-bonded form, CN⋯H may serve as a surrogate CO ligand in its ability to delocalize electron density.

Notably, metals can also be captured by the electron rich iron–sulfide anion (Fig. 12) [72]. In this diversity of S-based reactivity, the dianionic complex **21** resembles neutral dithiolato nickel(II) complexes, including the heterobimetallics based on (bme-daco)Ni^{II} shown as structures **7–10**.

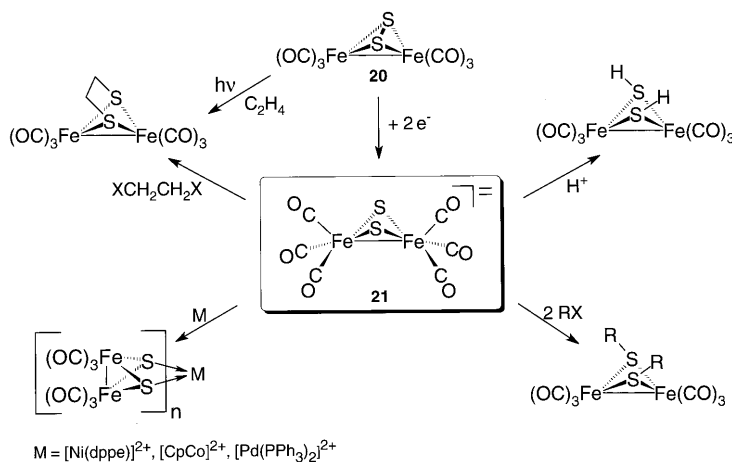


Fig. 12. Examples of reactivity of the Fe_2S_2 cores. See text for Refs.

4. Functional and theoretical modeling of [MFe] hydrogenases

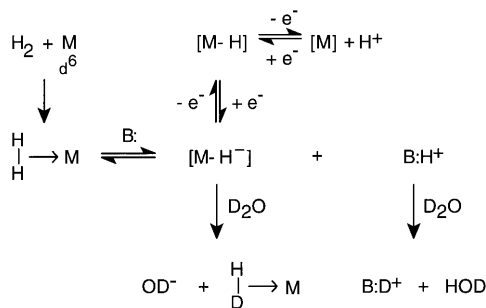
4.1. Homolytic and heterolytic cleavage mechanisms for dihydrogen activation by metals

The possibilities for H_2 activation by transition metals known to organometallic chemists are as follows: (1) Homolytic cleavage via oxidative addition to metals with easily accessible $n + 2$ oxidation states, primarily second and third row d^8 metals, producing metal dihydrides. (2) Homolytic cleavage via dinuclear oxidative addition to metal–metal bonded compounds, resulting in metal hydrides where the oxidation state of each metal has increased by $+1$. (3) Heterolytic cleavage via the metal induced acid character of dihydrogen in $(\eta^2\text{-H}_2)\text{M}$ complexes [73–75]. It is generally accepted that the conditions suitable for the first two processes are also conducive to the binding of unsaturated molecules, such as olefins or CO, and subsequent insertions to produce $\text{M}-\text{C}-\text{H}$ bonds followed by reductive $\text{H}-\text{C}-\text{H}$ eliminations — i.e. hydrogenation catalysis. The latter heterolysis however, polarizes the bonding electron pair of dihydrogen, generating an anionic $\text{M}-\text{H}^-$ site, suitable for hydride nucleophilic attack reactivity, or electron transfer. It is the electron-transfer process that is appropriate to hydrogenases. Of course the reverse of H_2 activation thus described is H_2 production.

That the activation of H_2 in hydrogenases occurs by a heterolytic process was suggested a half-century ago from pH-dependent kinetic studies of $[\text{NiFe}]\text{H}_2$ ase enzyme activity [76]. Even earlier it was established that H_2 ase could catalyze H/D exchange between gaseous D_2 and H_2O [77]. Since then the H/D exchange reaction has become a useful monitor of enzyme activity in the absence of electron donors/acceptors.

It should be noted that H/D exchange activity is not a ‘smoking gun’ for a heterolytic H_2 activation mechanism since both $(\eta^2\text{-H}_2)\text{M}$ and $\text{H}-\text{M}$ complexes may undergo H/D exchange with D_2O . For example, $\text{HCo}(\text{CO})_4$ (as produced in the dinuclear oxidative addition reaction: $\text{H}_2 + \text{Co}_2^0(\text{CO})_8 \rightarrow 2\text{HCo}^1(\text{CO})_4$) is a strong acid, and easily exchanges $\text{Co}-\text{H}$ to $\text{Co}-\text{D}$ in D_2O .

For the process of $\eta^2\text{-H}_2$ binding, heterolytic splitting, and stable metal hydride formation, octahedrally coordinated, d^6 metals work best [78]. While some π -back donation from the metal stabilizes $\eta^2\text{-H}_2$ binding, excessive electron density on the metal leads to oxidative addition and homolytic cleavage. Furthermore, electron withdrawing ligands or good π -back-bonding ligands produce a stronger acid character for the $(\eta^2\text{-H}_2)\text{M}$ complex [79] and help stabilize the resultant anionic $\text{M}-\text{H}^-$ moiety produced after deprotonation. Thus, the myriad of $(\eta^2\text{-H}_2)\text{M}$ complexes now known [80] are typically in a mixed-ligand environment, and the acidity of the metal-bound dihydrogen is highly sensitive to ligand [73]. Both $[\text{NiFe}]\text{H}_2$ ase and Fe-only H_2 ase find such a d^6 metal, Fe^{II} , in a ligand environment which may be tuned to facilitate $\eta^2\text{-H}_2$ binding or release. Thus, it is reasonable to invoke a uni-centered $(\eta^2\text{-H}_2)\text{Fe}$ activation process, as shown in H/D exchange activity in Scheme 4. It is the anionic $\text{M}-\text{H}^-$ that harnesses or controls the electrons or reducing ability of hydrogen and provides a path for electron transfer.



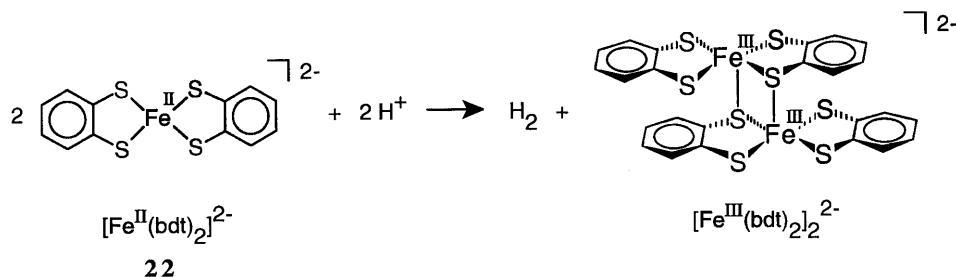
Scheme 4.

To observe such intermediates within a catalytic cycle as presented in Scheme 4 is the goal of spectroscopists who probe the enzyme under various conditions. For example, an early (1991) ENDOR experiment on $[\text{NiFe}] \text{H}_2$ ase detected two types of exchangeable protons, derivable from H_2 , in different enzyme states and was interpreted in terms of a single Ni ion in the active site [81]. That study has been revisited in light of the now known heterobimetallic character of the $[\text{NiFe}]$ active site. Hoffman et al. conclude that this site in the Ni–A redox state is a novel $\text{Ni}^{\text{III}}\text{Fe}^{\text{II}}$ trapped valence cluster [82]. Such spectroscopic studies are key to providing a basis for models of catalysis and indeed the theoretical models presented below use $\text{Ni}^{\text{III}}\text{Fe}^{\text{II}}$ in their calculations.

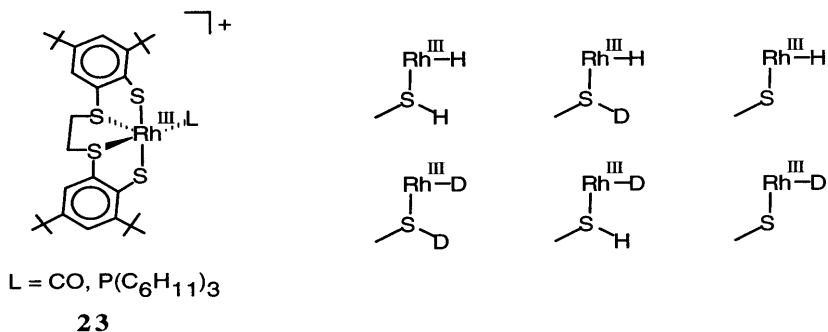
4.2. Functional models for heterolytic H_2 cleavage

An appropriate functional model for Fe-only hydrogenase lies in the synthesis of the $(\mu\text{-pdt})\text{Fe}_2(\text{CO})_6$ compound from the dithiol and either $\text{Fe}_2(\text{CO})_9$ or $\text{Fe}_3(\text{CO})_{12}$ releasing H_2 as two Fe(0) atoms are oxidized to Fe(I), maintaining an Fe–Fe bond, as expressed in Scheme 3. No designed functional heterobimetallic model exists for $[\text{NiFe}]$ hydrogenase. While several studies of monometallic compounds show aspects of the chemistry required for H_2 ases, we have chosen examples from only two laboratories to present below.

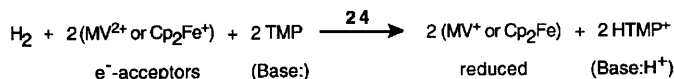
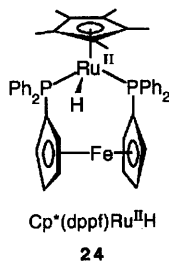
Sellman and coworkers have shown that a thiolate rich d^6 Fe^{II} complex of 1,2-benzene dithiolate, complex **22**, reacts with acid to generate H_2 and the oxidized Fe(III) dimeric complex as shown below. An ill-characterized, blue–gray intermediate was presumed to contain Fe–H or Fe–SH [83].



Further model studies by Sellman's group using the d^6 Rh^{III} complex **23** shown below found some catalytic activity for heterolytic H_2 cleavage including H^+/D_2 exchange using EtOH as a proton source [84]. For the H/D exchange process all possible metal thiolate hydrogenates or deuterates were characterized by NMR, however the expected $\eta^2\text{-H}_2$ or $\eta^2\text{-D}_2$ intermediates were not stable or observed [84].

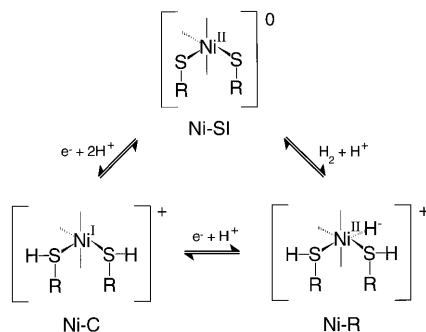


The $\text{Cp}^*(\text{dppf})\text{Ru}^{\text{II}}\text{H}$ complex **24** (dppf = (bis(diphenylphosphino)ferrocene)) has been developed by Hembre et al. as a functional model for $[\text{NiFe}]$ hydrogenase [85]. Although **24** contains two metals, only Ru is redox active while the Fe is merely a part of the dppf ligand. This model is unique in that it demonstrates the sequential single electron-transfer processes of H_2 ases. The $\text{Cp}^*(\text{dppf})\text{Ru}^{\text{II}}\text{H}$ complex **24** catalyzes the stepwise oxidation of H_2 in the presence of single electron acceptors (methyl viologen, MV^{2+} , or ferrocinium, Fc^+) and a base. The design of this model is critical as the requirement of a base for H^+ removal from the presumed $\eta^2\text{-H}_2$ complex must be met with a sterically hindered base such as tetramethylpiperidine, TMP, otherwise the base will interfere with $\eta^2\text{-H}_2$ binding to the metal. The unusual dppf ligand also prevents side reactions of the Ru-H by blocking intermolecular pathways. Bulk chemical oxidation proved the $\text{Ru}(\text{II})$ complex **24** could be oxidized to a stable 17-electron $[\text{Cp}^*(\text{dppf})\text{Ru}^{\text{III}}\text{H}]^+$ species; the latter complex was characterized by atom abstraction reactions with dihalogens to give the $[\text{Cp}^*(\text{dppf})\text{Ru}^{\text{IV}}\text{-(H)(X)}]^+$ complexes [85]. Again, the $\eta^2\text{-H}_2$ complex expected as an intermediate was not observed, however the inhibitory effect of CO, was offered as evidence of an open site requirement. A detailed mechanism has not been established.



4.3. Theoretical models for [NiFe] hydrogenase

Prior to the first crystal structure report of a [NiFe] hydrogenase, mechanistic models for H₂ uptake/evolution in [NiFe]H₂ases focused on nickel and nickel thiolates as H₂ activation sites, typically evoking S-cysteine as an internal base for intramolecular heterolytic H₂ cleavage, producing a Ni^{II}–H[–] and nickel-bound cysteinol as shown in Scheme 5 [86]. Appeal of this proposed mechanism remained even after the dinuclear active site was established in that the Ni(S-cysteine)₂ is at the entrance of the active site of [NiFe]H₂ase, and is well positioned to receive H₂ from the gas access channel [87].



Scheme 5.

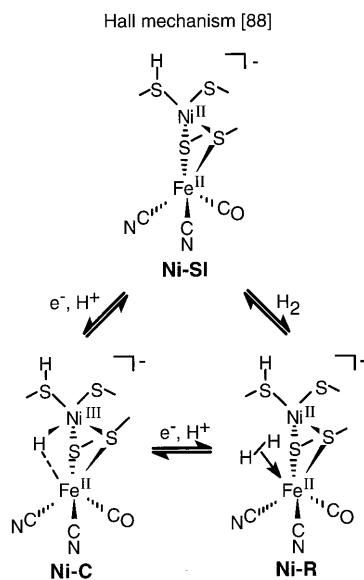
Currently there is no experiment that could disprove the Lindahl mechanism, Scheme 5, although most current models based on spectroscopies [6] or theory (vide infra) use Ni^{III} to account for the odd electron species. From it we might conjecture that the purpose of the second metal, i.e. the Fe(CN)₂(CO) unit in the back of the Ni active site is to moderate the ligand environment about nickel to facilitate its binding ability to dihydrogen. Cammack's attractive modification of the Lindahl mechanism uses the nickel–iron site in tandem, generating an iron hydride following initial H₂ capture by nickel [2]. Both proposals are speculative and do not invoke the most prominent feature of the functional models of heterolytic H₂ activation described above, i.e. the presence of the d⁶ iron and its capability to bind dihydrogen in η²-H₂–M complex formation.

The advent of the [NiFe] and [Fe-only]H₂ase crystal structure determinations, the realization that similar Fe(CO)(CN)_x moieties are present in the active sites of all such H₂ases, as well as the connection between the low spin d⁶ metal ion and well-known η²-H₂ complexes have engaged the interest of several theoretical groups. While a full discussion of the current theoretical work is not warranted here, a brief presentation is offered to promote the synergism between functional modeling and theory.

The practicalities of computation time on large protein molecules necessitates limits be placed on the active site and its environment. Given the extent of H-bonding to cyanide in the active sites, spatial orientations as found in the crystal structure are expected to be largely maintained. The four theoretical studies of $[\text{NiFe}] \text{H}_2\text{ase}$ thus far [88–91] have employed density functional theory (DFT) calculations. Current versions largely restrict ligand motion (although some folding of the dinuclear active site occurs); and, all have relied on results of one or more experimental techniques as a baseline for their calculations. Key points agreed upon in all the studies are as follows:

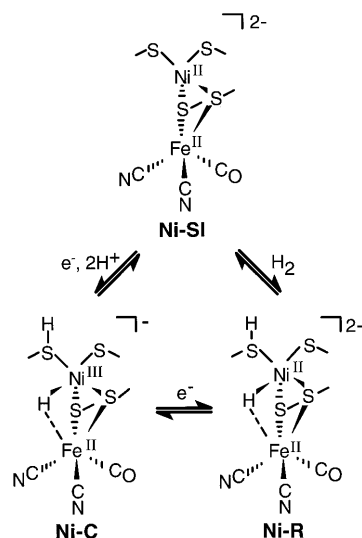
1. The bridging oxo ligand must be lost prior to catalytic activity.
2. During the reduction process, the active site ‘folds’, resulting in a decrease of the Ni–Fe distance, consistent with the contraction observed in the structure of the reduced $[\text{NiFeSe}] \text{H}_2\text{ase}$ relative to that of the oxidized $[\text{NiFe}] \text{H}_2\text{ase}$.
3. At some point in the catalytic cycle, a bridging hydride species is formed either prior to or as a result of the active site folding.
4. The iron site is not redox active and remains as Fe(II) in all spectroscopically defined redox states of the enzyme.

The mechanisms of $[\text{NiFe}] \text{H}_2\text{ase}$ proposed by Hall [88] and De Gioia [89] (Schemes 6 and 7) are similar, but differ in the way that they were derived and in a few key steps along the catalytic pathway. The De Gioia mechanism is based upon one first proposed by Dole [92] in which the significance of enzymic redox states is correlated with EPR results and the original interpretation of nickel oxidation states. The Hall mechanism uses computations of energy-minimized ‘candidate’ structures for each redox state of the enzyme that are referenced to the



Scheme 6.

Dole [92], De Gioia [89] mechanism



Scheme 7.

IR stretching frequencies of the enzyme in those states and standardized to organometallic model compounds which contain an $Fe(CO)(CN)_2$ unit [34]. The most reasonable candidate structures were then combined to suggest a reaction path. The proposed Ni–C states are exactly the same in the two mechanisms with major differences in the Ni–SI and Ni–R states. The De Gioia mechanism has a -2 charge on the complex in the Ni–SI and Ni–R states, but according to Hall both states have a protonated terminal cysteine residue to yield an overall -1 charge. Addition of H_2 to the Ni–R state is expressly described as a dihydrogen adduct at the iron site by Hall, whereas its intermediacy could be inferred but is not expressly described as such by DeGioia, who suggests a bridging hydride species is produced in this step.

Other studies provide insight into what may be needed to better model the enzyme. By using calculated minimum activation barriers to propose structures for the catalytic cycle, Pavlov et al. finds that the charge on the complex being modeled has a significant influence on the mechanism [90]. A combination of quantum mechanical and molecular mechanics to model the active site and the effects of the protein, respectively, found a significant effect of the protein matrix [91]. Another study by De Gioia found that there is very little if any electronic change between the active sites of $[NiFe]$ and $[NiFeSe]H_2ase$ and suggests that the enhanced reactivity of the $[NiFeSe]H_2ase$ is due to some difference in the protein environment [93].

5. Comments

The goal of this review was to provide an overview of the organometallic coordination chemistry appropriate to develop understanding of the remarkable discovery of the $\text{Fe}(\text{CO})(\text{CN})_x$ unit in NiFe and Fe-only hydrogenases. It might appear that the many fundamentally important biophysical and biochemical studies that preceded the six protein crystal structures of NiFe and Fe-only hydrogenases have been slighted or taken for granted. We would maintain that where new interpretation of prior results is needed, the original researchers, rather than we, are ultimately more qualified to do so. The elucidation of the molecular structures and the spectroscopic verification of diatomic ligands as active site construction units creates, however, a research opportunity for which organometallic chemists are uniquely suited to explore. It also predilects our interpretation in terms of low valent iron chemistry.

Certainly CO and CN^- have been used as biological probe molecules for decades, introduced as inhibitors or spectroscopic handles; indeed, vibrational spectroscopy of diatomics in metallobiomolecules is a well-developed field. Thus the power of this application, which brings with it the capability to observe enzyme states less or non-accessible to other techniques, will be brought to bear on a problem of long standing in the organometallic community. The problem lies in the identification of the intermediates and mechanisms of bimetallic, heterobimetallic, or cluster catalysis. The enzyme isolates and protects those sites from aggregation or degradation. Through the years the catalysis and organometallic community of scientists have attempted the same through various approaches, but never with the clear success of these natural systems. The synergy of biology and theoretical, functional, and structural modeling provides a serious opportunity to develop understanding of the roles of all components, including the protein matrix itself.

Acknowledgements

The authors express appreciation to the National Science Foundation (CHE 9812355) for funding contributions to their original work in this area. A National Institutes of Health Training grant T32-GM08523 (Graduate Training in Biological Chemistry) provided support for E.J.L. Helpful discussion with Professors Michael B. Hall and Paul Lindahl is greatly appreciated.

References

- [1] M.W.W. Adams, E.I. Stiefel, *Science* 282 (1998) 1842.
- [2] R. Cammack, P. van Vliet, in: J. Reedijk (Ed.), *Bioinorganic Catalysis*, 2nd ed., Marcel Dekker, New York, 1999, p. 231.
- [3] M. Frey, *Struct. Bond.* 90 (1998) 97.
- [4] R.K. Thauer, A.R. Klein, G.C. Hartmann, *Chem. Rev.* 96 (1996) 3031.
- [5] A. Berkessel, R.K. Thauer, *Angew. Chem. Int. Ed. Engl.* 34 (1995) 2247.

- [6] M.J. Maroney, G. Davidson, C.B. Allan, J. Figlar, *Struct. Bond.* 92 (1998) 1.
- [7] J.C. Fontecilla-Camps, *Struct. Bond.* 91 (1998) 1.
- [8] M. Frey, J.C. Fontecilla-Camps, *Acc. Chem. Res.* (2000) in press.
- [9] J.J.G. Moura, M. Teixeira, I. Moura, J. LeGall, in: J.R. Lancaster Jr. (Ed.), *The Bioinorganic Chemistry of Nickel*, VCH Publishers, New York, 1988, pp. 191–226.
- [10] A. Volbeda, M.-H. Charon, C. Piras, E.C. Hatchikian, M. Frey, J.C. Fontecilla-Camps, *Nature* 373 (1995) 580.
- [11] A. Volbeda, E. Garcin, C. Piras, A.L. de Lacey, V.M. Fernandez, E.C. Hatchikian, M. Frey, J.C. Fontecilla-Camps, *J. Am. Chem. Soc.* 118 (1996) 12989.
- [12] E. Garcin, X. Vernede, E.C. Hatchikian, A. Volbeda, M. Frey, J.C. Fontecilla-Camps, *Structure* 7 (1999) 557.
- [13] Y. Higuchi, T. Yagi, N. Yasuoka, *Structure* 5 (1997) 1671.
- [14] Y. Higuchi, H. Ogata, K. Miki, N. Yasuoka, T. Yagi, *Structure* 7 (1999) 549.
- [15] J.W. Peters, W.N. Lanzilotta, B.J. Lemon, L.C. Seefeldt, *Science* 282 (1998) 1853.
- [16] Y. Nicolet, C. Piras, P. Legrend, C.E. Hatchikian, J.C. Fontecilla-Camps, *Structure* 7 (1999) 13.
- [17] K.A. Bagley, C.J. Van Garderen, M. Chen, E.C. Duin, S.P.J. Albracht, W.H. Woodruff, *Biochemistry* 33 (1994) 9229.
- [18] M.W.W. Adams, *Biochim. Biophys. Acta* 1020 (1990) 115.
- [19] R.P. Happe, W. Roseboom, A.J. Pierik, S.P.J. Albracht, K.A. Bagley, *Nature* 385 (1997) 126.
- [20] A.J. Pierik, W. Roseboom, R.P. Happe, K.A. Bagley, S.P.J. Albracht, *J. Biol. Chem.* 274 (1999) 3331.
- [21] A. Volbeda, E. Garcin, C. Piras, A.L. de Lacey, V.M. Fernandez, E.C. Hatchikian, M. Frey, J.C. Fontecilla-Camps, *J. Am. Chem. Soc.* 118 (1996) 12989.
- [22] A.L. de Lacey, E.C. Hatchikian, A. Volbeda, M. Frey, J.C. Fontecilla-Camps, V.M. Fernandez, *J. Am. Chem. Soc.* 119 (1997) 7181.
- [23] T.M. Van der Spek, A.F. Arendsen, R.P. Happe, S. Yun, K.A. Bagley, D.J. Stufkens, W.R. Hagen, S.P.J. Albracht, *Eur. J. Biochem.* 237 (1996) 629.
- [24] A.J. Pierik, M. Hulstein, W.R. Hagen, S.P.J. Albracht, *Eur. J. Biochem.* 258 (1998) 572.
- [25] Z. Gu, J. Dong, C.B. Allan, S.B. Choudhury, R. Franco, J.J.G. Moura, I. Moura, J. LeGall, A.E. Przybyla, W. Roseboom, S.P.J. Albracht, M.J. Axley, R.A. Scott, M.J. Maroney, *J. Am. Chem. Soc.* 118 (1996) 11155.
- [26] C.V. Popescu, E. Münck, *J. Am. Chem. Soc.* 121 (1999) 7877.
- [27] C. Bagyinka, J.P. Whitehead, M.J. Maroney, *J. Am. Chem. Soc.* 115 (1993) 3576.
- [28] C.E. Coffey, *J. Inorg. Nucl. Chem.* 25 (1963) 179.
- [29] D.J. Darensbourg, J.H. Reibenspies, C.-H. Lai, W.-Z. Lee, M.Y. Darensbourg, *J. Am. Chem. Soc.* 119 (1997) 7903.
- [30] C.-H. Lai, W.-Z. Lee, M.L. Miller, J.H. Reibenspies, D.J. Darensbourg, M.Y. Darensbourg, *J. Am. Chem. Soc.* 120 (1998) 10103.
- [31] W.P. Fehlhammer, M. Fritz, *Chem. Rev.* 93 (1993) 1243.
- [32] S.A. Goldfield, K.N. Raymond, *Inorg. Chem.* 13 (1974) 770.
- [33] M.Y. Darensbourg, H.L.C. Barros, *Inorg. Chem.* 18 (1979) 3286.
- [34] D. Sellmann, T. Becker, F. Knoch, *Chem. Eur. J.* 2 (1996) 1092.
- [35] D. Sellmann, G. Mahr, F. Knoch, M. Moll, *Inorg. Chim. Acta.* 224 (1994) 45.
- [36] H.-F. Hsu, S.A. Koch, C.V. Popescu, E. Münck, *J. Am. Chem. Soc.* 119 (1997) 8371.
- [37] D.H. Nguyen, H.-F. Hsu, M. Millar, S.A. Koch, C. Achim, E.L. Bominaar, E. Münck, *J. Am. Chem. Soc.* 118 (1996) 8963.
- [38] P.J. Schebler, C.G. Riordan, I.A. Guzei, A.L. Reingold, *Inorg. Chem.* 37 (1998) 4754 and Refs. therein.
- [39] W.-F. Liaw, Y.-C. Horng, D.-S. Ou, C.-Y. Ching, G.-H. Lee, S.-M. Peng, *J. Am. Chem. Soc.* 119 (1997) 9299 and Refs. therein.
- [40] R.P. Happe, W. Roseboom, S.P.J. Albracht, *Eur. J. Biochem.* 259 (1999) 602.
- [41] M. Kumar, S.W. Ragsdale, *J. Am. Chem. Soc.* 114 (1992) 8713.
- [42] C.-H. Lai, J.H. Reibenspies, M.Y. Darensbourg, *Angew. Chem. Int. Ed. Engl.* 35 (1996) 2390.

- [43] D.K. Mills, Y.-M. Hsiao, P.J. Farmer, E.V. Atnip, J.H. Reibenspies, M.Y. Darensbourg, *J. Am. Chem. Soc.* 113 (1991) 1421.
- [44] G.T. Musie, PhD Dissertation, Texas A&M University, 1997.
- [45] G.J. Colpas, R.O. Day, M.J. Maroney, *Inorg. Chem.* 31 (1992) 5053.
- [46] F. Osterloh, W. Saak, D. Hasse, S. Pohl, *J. Chem. Soc. Chem. Commun.* (1997) 979.
- [47] W.-F. Liaw, C.-Y. Chiang, G.-H. Lee, S.-M. Peng, C.-H. Lai, M.Y. Darensbourg, *Inorg. Chem.* 39 (2000) 480.
- [48] G. Musie, P.J. Farmer, T. Tuntulani, J.H. Reibenspies, M.Y. Darensbourg, *Inorg. Chem.* 35 (1996) 2176.
- [49] D. Seyferth, R.S. Henderson, L.-C. Song, *Organometallics* 1 (1982) 125.
- [50] C.H. Wei, L.F. Dahl, *Inorg. Chem.* 4 (1965) 1.
- [51] R. Rossetti, G. Gervasio, P.L. Stanghellini, *Inorg. Chim. Acta* 35 (1979) 73.
- [52] J.A. de Beer, R.J. Haines, R. Greatrex, N.N. Greenwood, *J. Chem. Soc. A* (1971) 3271.
- [53] B.K. Teo, M.B. Hall, R.F. Fenske, L.F. Dahl, *Inorg. Chem.* 14 (1975) 3103.
- [54] R.B. King, *J. Am. Chem. Soc.* 84 (1962) 2460.
- [55] D. Seyferth, R.S. Henderson, L.-C. Song, *J. Organomet. Chem.* 192 (1980) C1.
- [56] D. Seyferth, G.B. Womack, M.K. Gallagher, M. Cowie, B.W. Hames, J.P. Fackler, A.M. Mazany, *Organometallics* 6 (1987) 283.
- [57] A. Winter, L. Zsolnai, G. Huttner, *Z. Naturforsch* 37b (1982) 1430.
- [58] E.J. Lyon, I.P. Georgakaki, J.H. Reibenspies, M.Y. Darensbourg, *Angew. Chem. Int. Ed. Engl.* 38 (1999) 3178.
- [59] M.A. Schmidt, S.M. Contakes, T.B. Rauchfuss, *J. Am. Chem. Soc.* 121 (1999) 9736.
- [60] R.B. English, L.R. Nassimbeni, M.F. Philpott, *Acta Crystallogr.* B34 (1978) 2304.
- [61] D. Seyferth, G.B. Womack, C.M. Archer, J.C. Dewan, *Organometallics* 8 (1989) 430.
- [62] W.-F. Liaw, N.-H. Lee, C.-H. Chen, C.-M. Lee, G.-H. Lee, S.-M. Peng, *J. Am. Chem. Soc.* 122 (2000) 488.
- [63] S. Aime, G. Gervasio, R. Rossetti, P.L. Stanghellini, *Inorg. Chim. Acta* 40 (1980) 131.
- [64] P.C. Ellgen, J.N. Gerlach, *Inorg. Chem.* 12 (1973) 2526.
- [65] M. Basato, *J. Chem. Soc. Dalton Trans.* (1975) 911.
- [66] P.M. Treichel, R.A. Crane, R. Matthews, K.R. Bonnin, D. Powell, *J. Organomet. Chem.* 402 (1991) 233.
- [67] N.J. Taylor, M.S. Arabi, R. Mathieu, *Inorg. Chem.* 19 (1980) 1740.
- [68] J.-M. Savariault, J.-J. Bonnet, R. Mathieu, J. Galy, C. R. Acad. Sci. Paris 284 (1977) 663.
- [69] J. Messelhäuser, K.U. Gutensohn, I.-P. Lorenz, W. Hiller, *J. Organomet. Chem.* 321 (1987) 377.
- [70] C.J. Casewit, R.C. Haltiwanger, J. Noordik, M.R. Dubois, *Organometallics* 4 (1985) 119.
- [71] D. Seyferth, R.S. Henderson, *J. Organomet. Chem.* 218 (1981) C34.
- [72] D.E. Barber, M. Sabat, E. Sinn, B.A. Averill, *Organometallics* 14 (1995) 3229.
- [73] R.H. Morris, *Inorg. Chem.* 31 (1992) 1471.
- [74] E.P. Cappellani, S.D. Drouin, G. Jia, P.A. Maltby, R.H. Morris, C.T. Schweitzer, *J. Am. Chem. Soc.* 116 (1994) 3375.
- [75] T.A. Luther, D.M. Heinekey, *Inorg. Chem.* 37 (1998) 127.
- [76] A.I. Krasna, D. Rittenberg, *J. Am. Chem. Soc.* 76 (1954) 3015.
- [77] A. Farkas, L. Farkas, J. Yudkin, *Proc. R. Soc. (London)* B115 (1934) 373.
- [78] G.J. Kubas, *Acc. Chem. Res.* 21 (1988) 120.
- [79] R.H. Crabtree, *Acc. Chem. Res.* 23 (1990) 95.
- [80] F.A. Cotton, G. Wilkinson, C.A. Murillo, M. Bochmann, in: *Advanced Inorganic Chemistry*, 6th ed., John Wiley and Sons, New York, 1999 and Refs. therein.
- [81] C. Fan, M. Teixeira, J. Moura, I. Moura, B.H. Huynh, J. LeGall, H.D. Peck Jr., B.M. Hoffman, *J. Am. Chem. Soc.* 113 (1991) 20.
- [82] J.E. Huyett, M. Carepo, A. Pamplona, R. Franco, I. Moura, J.J.G. Moura, B.M. Hoffman, *J. Am. Chem. Soc.* 119 (1997) 9291.
- [83] D. Sellmann, M. Geck, M. Moll, *J. Am. Chem. Soc.* 113 (1991) 5259.
- [84] D. Sellmann, G.H. Rackelmann, F.W. Heinemann, *Chem. Eur. J.* 3 (1997) 2071.
- [85] R.T. Hembre, J.S. McQueen, V.W. Day, *J. Am. Chem. Soc.* 118 (1996) 798.

- [86] L.M. Roberts, P.A. Lindahl, *Biochemistry* 33 (1994) 14339.
- [87] Y. Montet, P. Amara, A. Volbeda, X. Vernede, E.C. Hatchikian, M.J. Field, M. Frey, J.C. Fontecilla-Camps, *Nat. Struct. Biol.* 4 (1997) 523.
- [88] S. Niu, L.M. Thomson, M.B. Hall, *J. Am. Chem. Soc.* 121 (1999) 4000.
- [89] L. De Gioia, P. Fantucci, B. Guigliarelli, P. Bertrand, *Inorg. Chem.* 38 (1999) 2658.
- [90] M. Pavlov, M.R.A. Blomberg, P.E.M. Siegbahn, *Int. J. Quant. Chem.* 73 (1999) 197.
- [91] P. Amara, A. Volbeda, J.C. Fontecilla-Camps, M.J. Field, *J. Am. Chem. Soc.* 121 (1999) 4468.
- [92] F. Dole, A. Fournel, V. Magro, E.C. Hatchikian, P. Bertrand, B. Guigliarelli, *Biochemistry* 36 (1997) 7847.
- [93] L. De Gioia, P. Fantucci, B. Guigliarelli, P. Bertrand, *Int. J. Quant. Chem.* 73 (1999) 187.